Supporting Information

CNT serial copper-phenylacetylide to construct high-speed charge transfer/separation channels for effective photocatalytic degradation of PAHs

Hui-Ying Sun,[a]* Yue-Ying Xu[a], Bai-Ling Liu,[a]* Hua-Qiao Tan[b]*

[a] School of Chemistry and Environmental Engineering, Jilin Provincial Science and Technology Innovation Center of Optical Materials and Chemistry, Jilin Provincial International Joint Research Center of Photo functional Materials and Chemistry, Changchun University of Science and Technology, Changchun, 130022, China

[b] Key Laboratory of Polyoxometalate and Reticular Material Chemistry of Ministry of Education, Faculty of Chemistry, Northeast Normal University, Changchun, 130024, P. R. China

* Corresponding author:

E-mail: sunhuiying@cust.edu.cn; liubl563@cust.edu.cn; tanhq870@nenu.edu.cn

Table of Contents

1. Experimental Procedures

1.1 Characterization

Powder X-ray diffraction (XRD) patterns were gathered on a Bruker AXS D8 Focus with filtered Cu K_α radiation (λ = 1.54056 Å). The scanning electron microscope (SEM) images were acquired using the JEOL JSM 4800F SEM. Transmission electron microscopy (TEM), High-resolution images (HRTEM) and element maps were studied on a JEOL-2100F microscope with a 200 kV acceleration voltage. X-ray photoelectron spectroscopy (XPS) was recorded on ESCALABMKII spectrometer, using Al-K_α as achromatic X-ray source. UV-vis diffuse reflectance spectrum (DRS) was obtained by UV-2600 UV-Vis Spectrophotometer (Shimadzu) in which $BaSO_4$ as a reference sample. The N_2 adsorption-desorption isotherms were determined at 77 K by using a Quantachrome Autosorb iQ apparatus. Photoluminescence (PL) spectra were recorded by a high-resolution FLS 920 spectrofluorometer (Edinburgh Instruments). The electron paramagnetic resonance (EPR) measurements were carried out on a JEOL JES-FA200 spectrometer. The total organic carbon test was conducted on a German-analytikjena-multi N/C 3100.

1.2 Materials

$CuCl_2 \cdot 2H_2O$ (AR), methanol (99.7%), triethylamine (99%), phenylacetylene (98%), 1,4-diethynylbenzene (98%), ethanol (99.9%) were purchased from Shanghai Macklin Biochemical Technology Co., Ltd. Benzylamine and its derivatives, benzyl alcohol, thioanisole and acetonitrile were purchased from Aladdin Chemical Co., Ltd. All the chemicals were used as received without further purification.

$CuCl_2 \cdot 2H_2O$ (99.7%), methanol (99.7%), ethanol (99.5%), triethylamine (99%), phenylacetylene (98%), amino-modified CNT (>95%), naphthalene (99.7%), phenanthrene (97%) and pyrene (97%) were purchased from Shanghai Macklin Biochemical Technology Co., Ltd. All the chemicals were used as received without further purification.

1.3 Electrochemical impedance spectroscopy (EIS) and photocurrent measurements

All electrochemical tests were carried out by using a CHI660E workstation and performed at room temperature under atmospheric pressure. For EIS and photocurrent measurements, three electrode standard system was prepared in a quartz cell firstly. Pt plate, Ag/AgCl electrode and fluorine-doped tin oxide (FTO) glass deposited with samples were used as the counter electrode, the reference electrode and the working electrode respectively, and 0.1 M Na_2SO_4 aqueous solution was adopted as the electrolyte. Importantly, working electrode was prepared as follows: first, disperse 20 mg of the catalyst in 2 mL of absolute ethanol solution with 2.5% nafion to obtain a uniformly turbid liquid by ultrasonication for half an hour. Then, dropped the suspension was drip-coated on a 1 × 3 cm^2 FTO glass substrate to ensure the active area of the catalyst was about 2 cm^2. In the end, the obtained working electrode was dried at room temperature. For EIS experiments, frequency was set from 0.01 Hz to 10 kHz at 0 V sinusoidal ac-perturbation. A 300 W (CELHXF300, AULIGHT) xenon lamp with different bands monochromatic light was selected to carry out the photocurrent measurement. In order to reduce the effect of the experiments, the light source was irradiated from the back of the FTO.

1.4 Electron paramagnetic resonance (EPR) test

The EPR spectra of the samples were measured in the presence of 5,5-dimethyl-1-pyrroline N-oxide (DMPO). Before to determine the superoxide radicals (DMPO-·O_2^-) and hydroxyl radical (DMPO-·OH), 10.0 mg samples were dissolved in 0.5 mL methanol and water respectively, and then 50 mL DMPO was added with ultrasonic dispersion for 5 min. After irradiated for 3 min under visible light, the solution was subjected to analysis at room temperature. The typical signal of DMPO-·O_2^- and DMPO-·OH adducts indicate the generation of ·O_2^- and ·OH.

1.5 Evaluation methods of photocatalytic PAHs degradation

10 mg of photocatalyst was suspended in 20 mL of phenanthrene (PHE) aqueous solution ($C_{PHE} = 5.6 \times 10^{-5}$ M). After continuous stirring in the dark for 30 min to establish adsorption equilibrium, this system was exposed to visible light to initiate the photocatalytic reaction. A

300 W xenon lamp was used as the visible-light source. The photocatalysis system was cooled by circulating water and kept at 20 °C. Subsequently, 1 mL of the suspension was extracted every 5 min and filtered with filter membranes (aquo system) to remove the suspended catalyst. The absorbance of PHE was measured using a UV spectrophotometer in the characteristic 245 nm band. The degradation intermediates were extracted and analyzed using a GC-MS system equipped with 19091J-413 column (30 m × 0.32 mm). The chromatographic conditions were set with helium as the carrier gas at a flow rate of 1 mL/min, split less injection with an injection volume of 2 μL, and an injection temperature of 300 °C. The oven temperature was initially set at 60 °C and held for 1 min, then ramped up to 300 °C at a rate of 5 °C/min and held for 5 min. The photocatalytic degradation performance evaluation of naphthalene and pyrene is consistent with PHE.

1.6 Computational Details

All first-principles calculations were performed within the framework of DFT using the plane-wave pseudopotential approach as implemented in the Vienna Ab-initio Simulation Package (VASP) code[1-3]. The charge analysis of the catalyst was carried out using the Bader charge population method. A plane-wave basis set with a cutof energy of 400 eV and a Monkhorst-Pack scheme with a Gamma centered k-point were adopted in our calculations. The convergence standards of energy and force were selected as 10^{-4} eV and 0.03 eV/Å, respectively. In the reactive oxygen species calculation section, the formula for calculating oxygen adsorption energy is $E_{ads} = E_{total} – E_{cat.} - E_{oxygen\ molecule}$ ($E_{oxygen\ molecule}$ = -9.85 eV).

2. Results and Discussion

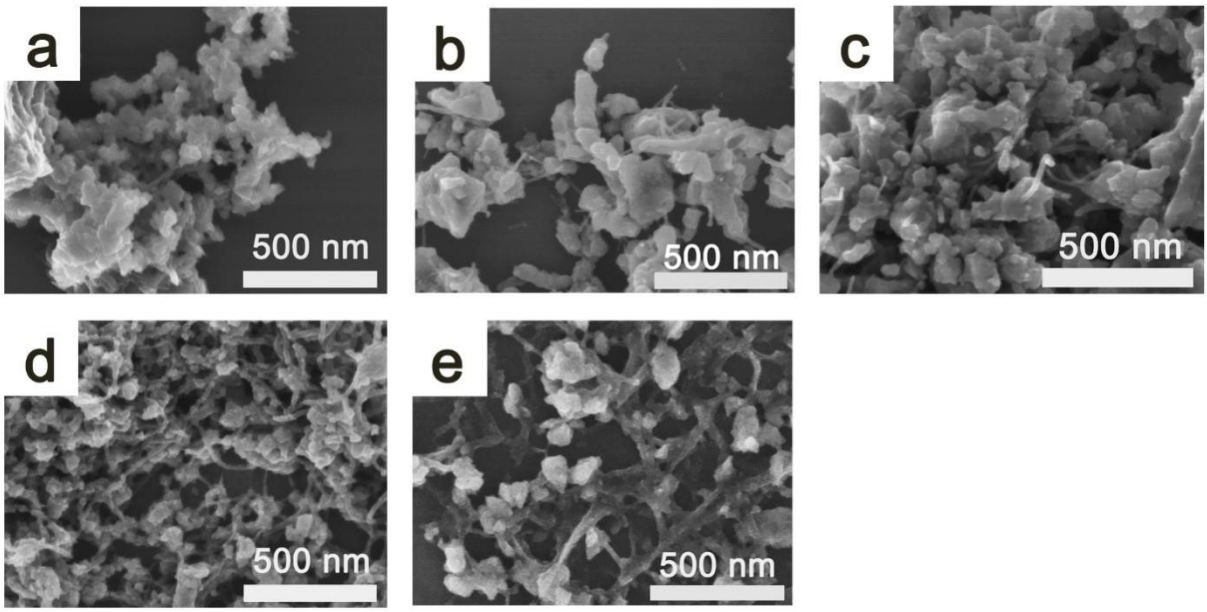

Figure S1. SEM images of (a) 1 wt% CNT-P, (b) 3 wt% CNT-P, (c) 5 wt% CNT-P, (d) 10 wt% CNT-P and (e) 15 wt% CNT-P.

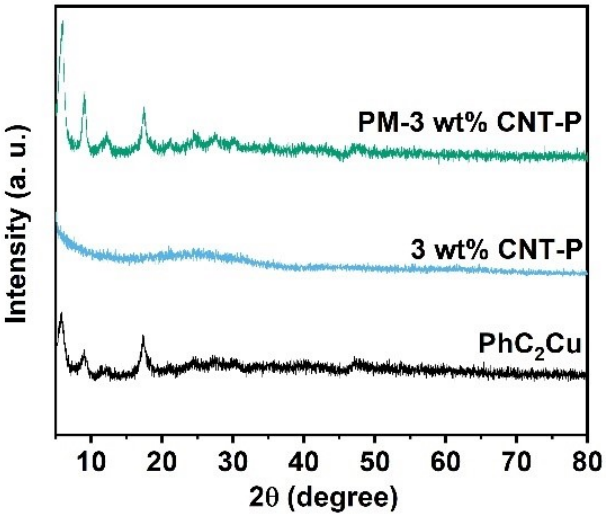

Figure S2. Powder XRD pattern of the samples.

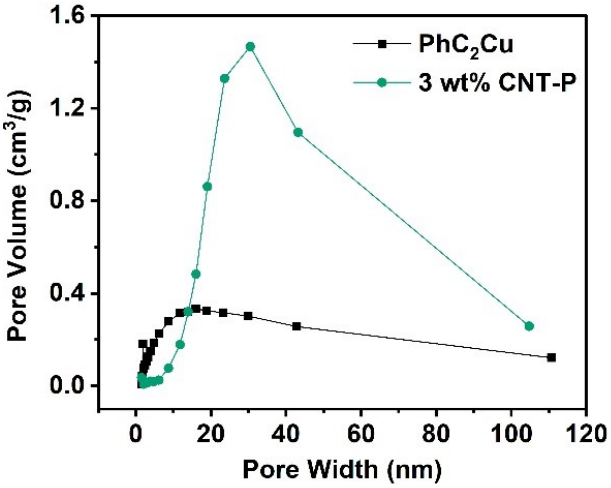

Figure S3. The pore size distribution of the samples.

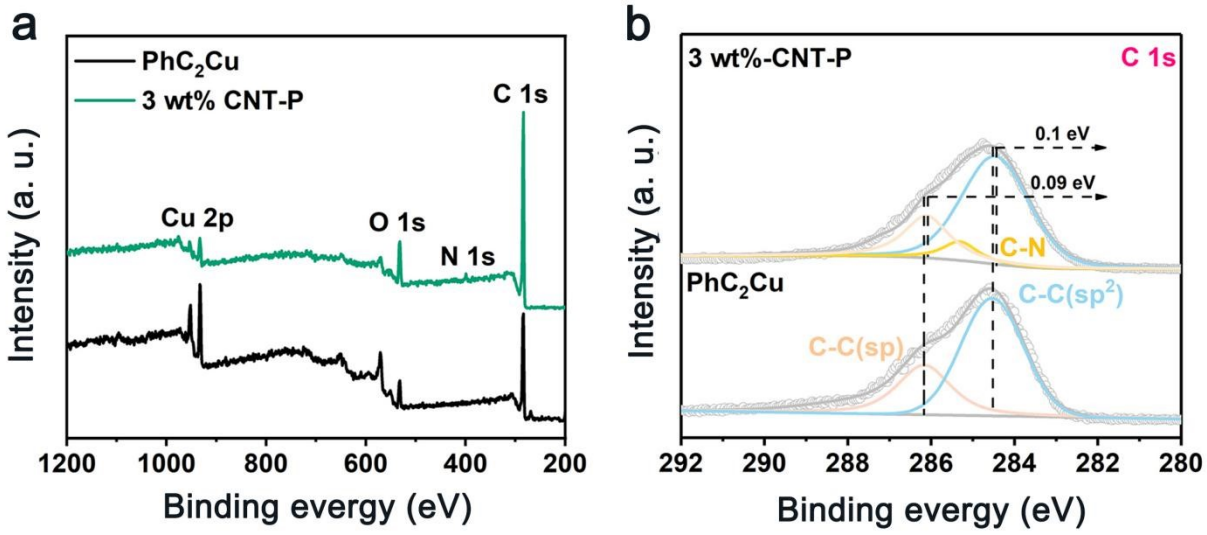

Figure S4. (a) XPS survey spectrum and (b) High-resolution XPS of C 1s spectra of the samples.

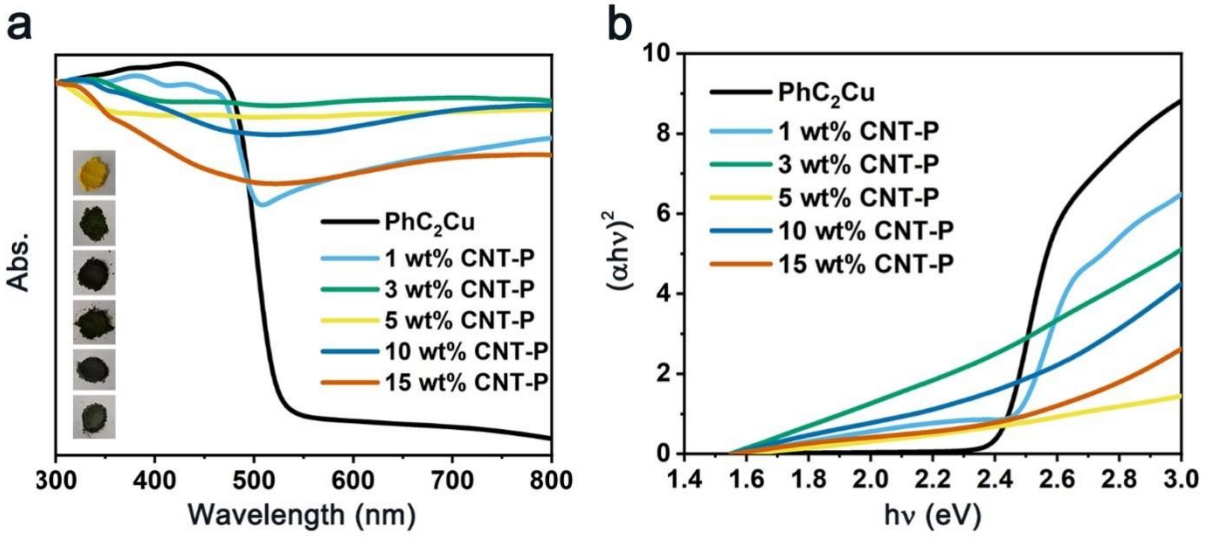

Figure S5. (a) Diffuse reflectance spectra (inset: the optical photos) and (b) The band gap energies transformed by Kubelka-Munk function of the samples.

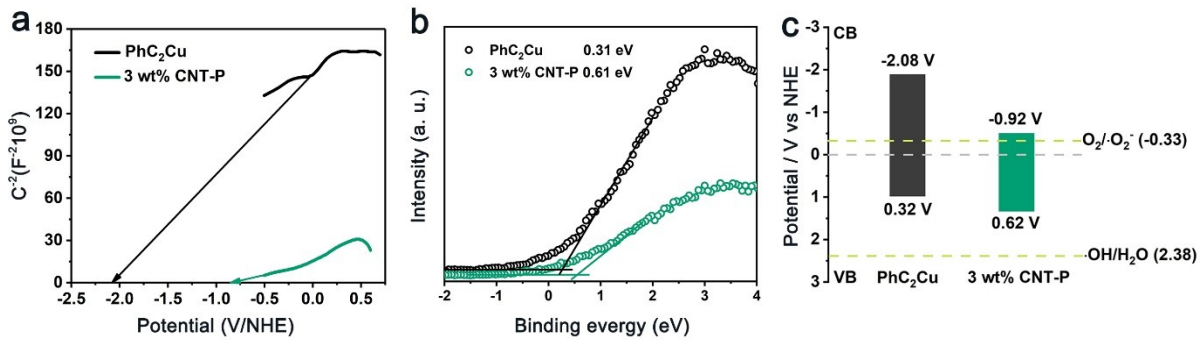

Figure S6. (a) Mott-Schottky plots, (b) VB-XPS and (c) Energy level of the samples.

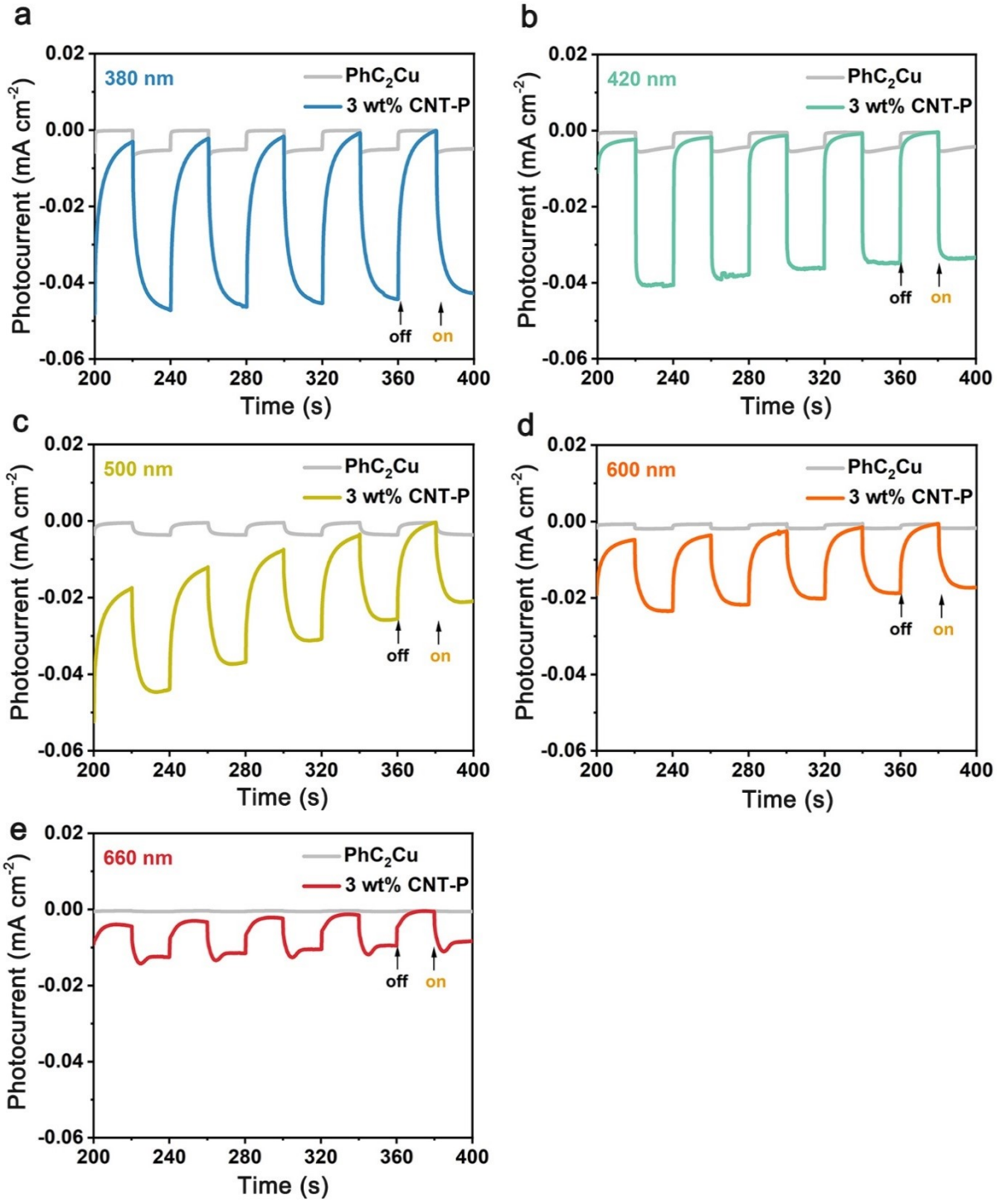

Figure S7. Transient photocurrents of the samples at different wavelength bands.

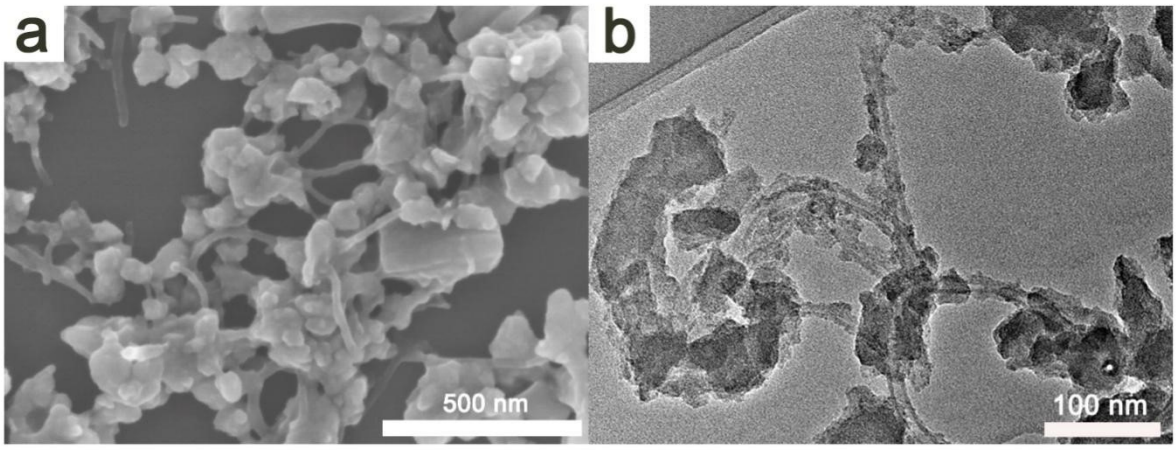

Figure S8. (a) SEM and (b) TEM images of 3 wt% CNT-P after photocatalytic PHE degradation.

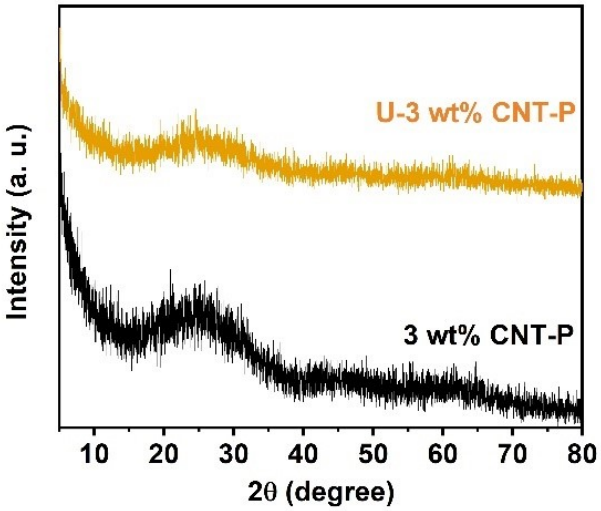

Figure S9. XRD spectra of the samples before and after the photocatalytic PHE degradation. The catalyst after circulation is marked as U-3 wt% CNT-P.

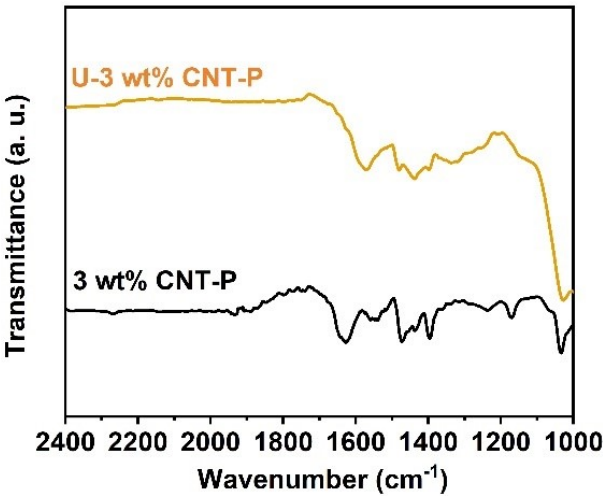

Figure S10. FTIR spectra of the samples before and after the photocatalytic PHE degradation.

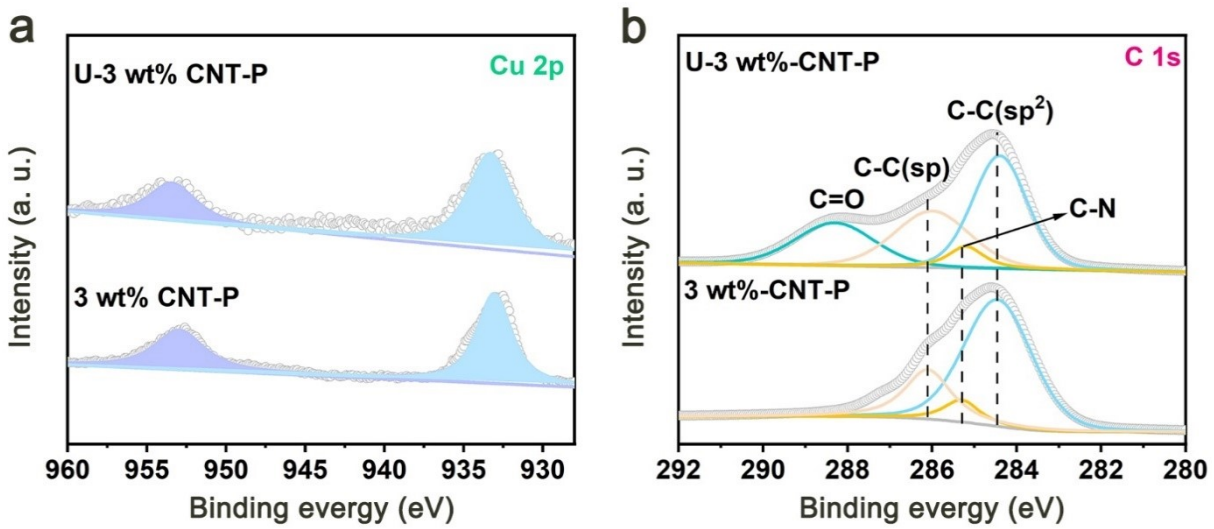

Figure S11. (a) Cu 2p and (b) C1s XPS spectra of the samples before and after the photocatalytic PHE degradation. The signal peak at 288.3 eV is attributed to residual degradation products.[4]

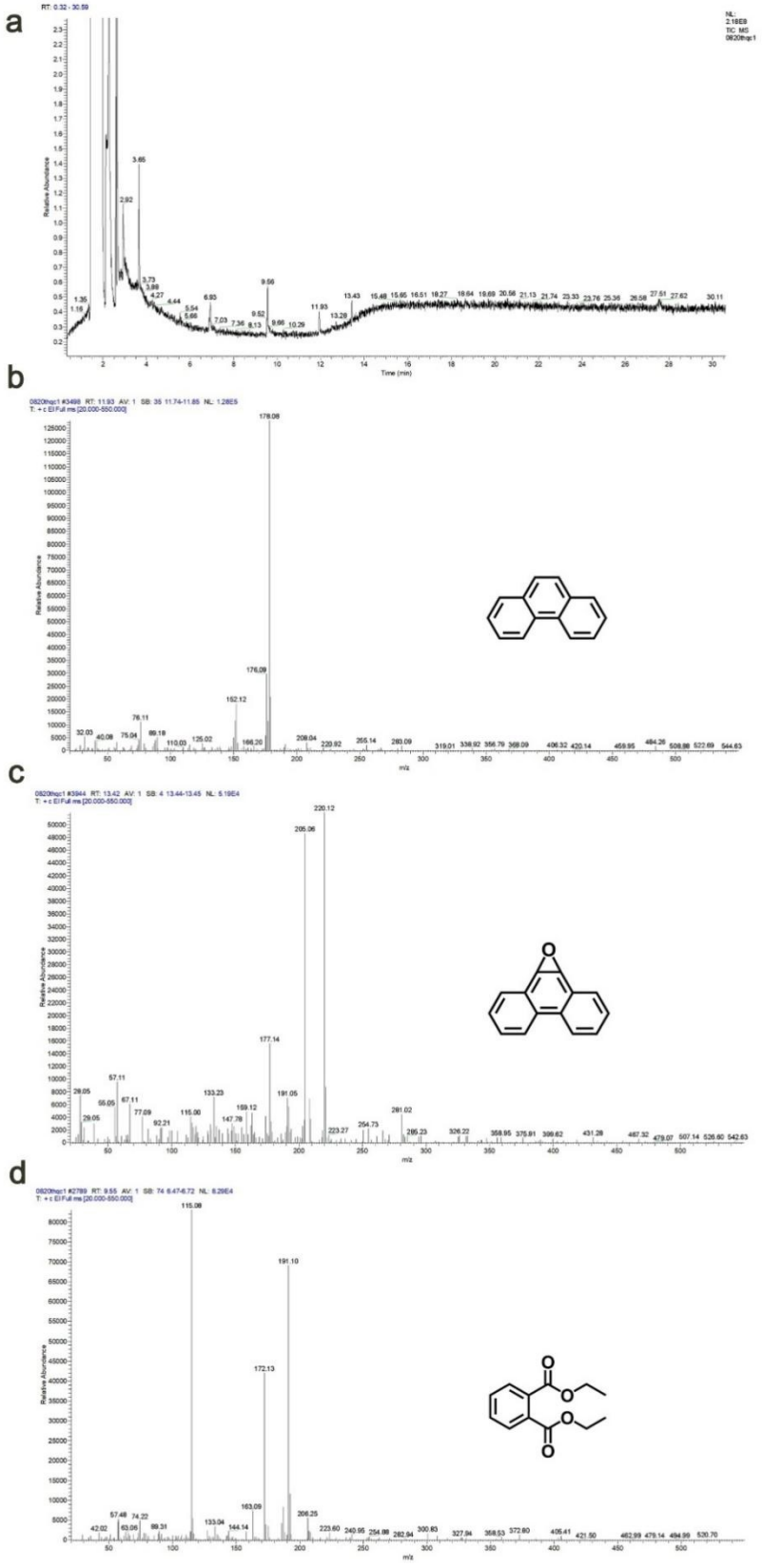

Figure S12. The main intermediate products generated during the process of photocatalytic PHE degradation by 3 wt% CNT-P.

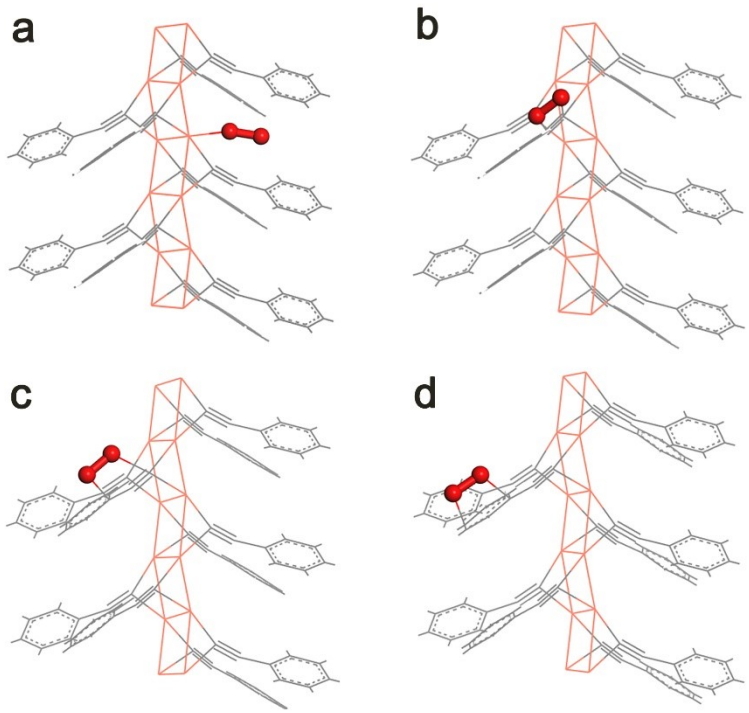

Figure S13. Schematic diagram of oxygen adsorption models at different sites of PhC_2Cu. In structural model, the gray, white, orange and red spheres represent C, H, Cu and O respectively. Oxygen molecules were dissociated at the adsorption site in Models b-d.

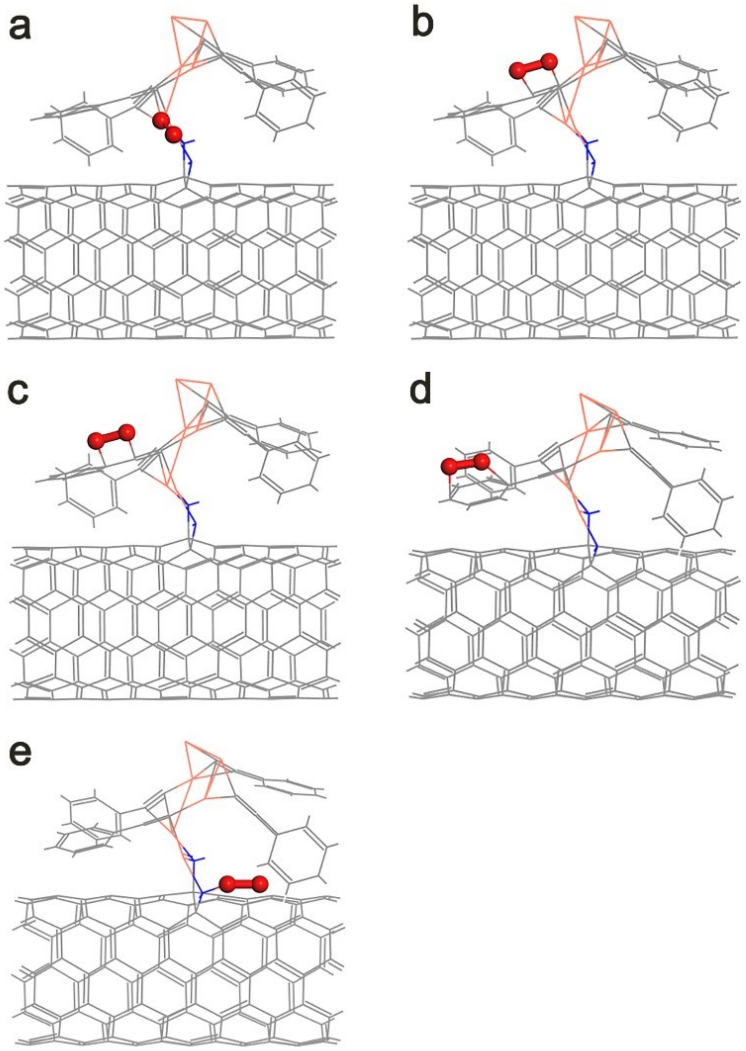

Figure S14. Schematic diagram of oxygen adsorption models at different sites of 3 wt% CNT-P. In structural model, the gray, white, orange and red spheres represent C, H, Cu and O respectively. Oxygen molecules were dissociated at the adsorption site in Models b-d. Oxygen molecules cannot adsorb at these positions in Models e after optimization.

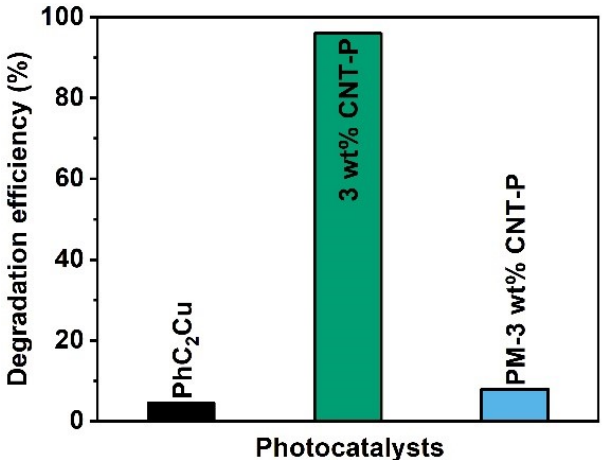

Figure S15. Degradation efficiency of naphthalene (100 ppm) by x wt% CNT-P with 70 min irradiation time.

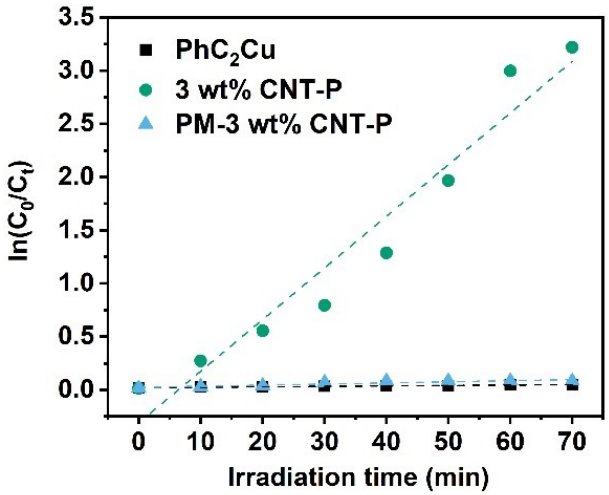

Figure S16. Kinetic linear fitting curves of photocatalytic naphthalene degradation by x wt% CNT-P.

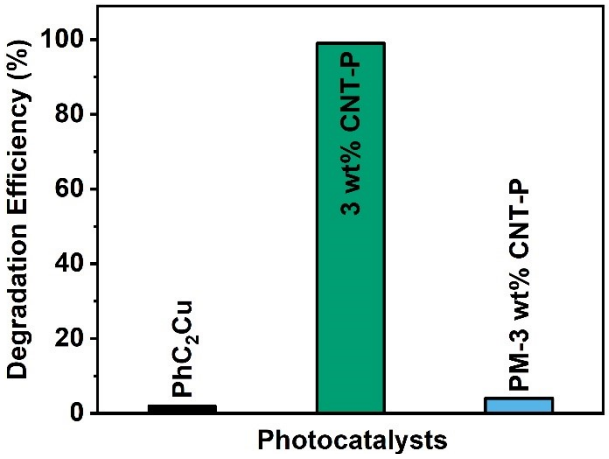

Figure S17. Degradation efficiency of pyrene by x wt% CNT-P with 50 min irradiation time.

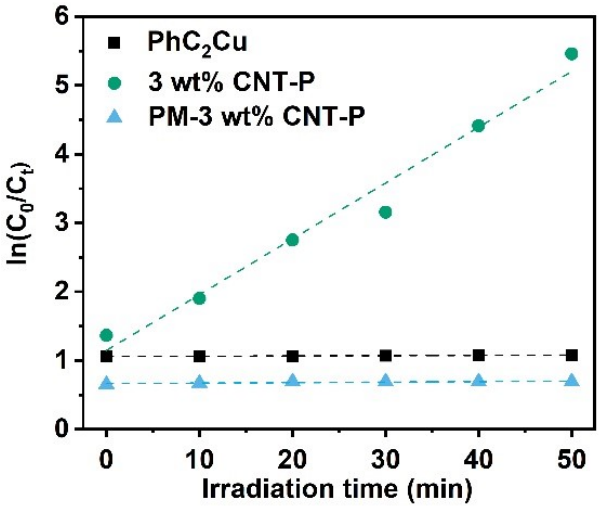

Figure S18. Kinetic linear fitting curves of photocatalytic pyrene degradation by x wt% CNT-P.

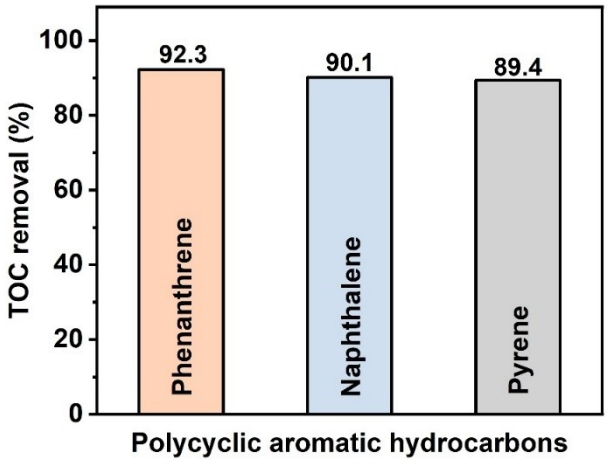

Figure S19. Total organic carbon (TOC) of different samples.

Table S1 EDX element analysis of x wt% CNT-P.

Samples	Element	Percentage by weight %	Percentage by atoms %
NH_2-CNT	C K	99.52	99.59
	N K	0.48	0.41
PhC_2Cu	C K	68.72	92.11
	Cu K	31.28	7.89
1 wt% CNT-P	C K	69.55	91.8
	Cu K	29.76	7.4
	N	0.69	0.8
3 wt% CNT-P	C K	71.55	92.4
	Cu K	27.56	6.7
	N	0.89	0.9
5 wt% CNT-P	C K	72.31	92.7
	Cu K	26.94	6.5
	N	0.75	0.8
10 wt% CNT-P	C K	73.55	93
	Cu K	25.75	6.2
	N	0.7	0.8
15 wt% CNT-P	C K	74.31	93.4
	Cu K	24.96	5.9
	N	0.73	0.7

Table S2 The conversion rate of the Glaser coupling reaction of the sample under light exposure.

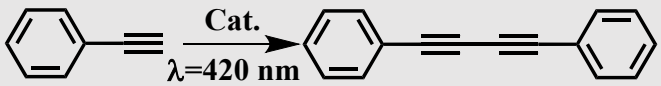

Entry	Cat.	Conv. [%]	Sel. [%]
1	PhC_2Cu	13	>99
2	3 wt% CNT-P	7	>99
3	15 wt% CNT-P	23	72[a]

[a]The reason for the selective reduction being lowered was that another organic compound, diphenylacetylene, was detected in the system.

Table S3 Optimized cell parameters and atomic coordinates of PhC_2Cu.

Space Group: $P2_1$ (C2-2) **a = 15.45 Å** **α = 90.00°** **b = 5.29 Å** **β = 109.23°** **c = 10.28 Å** **γ = 90.00°** **V = 793.22 Å^3**			
Cu1	0.5885	0.9706	0.6559
Cu2	0.5632	0.5043	0.5651
C1	0.9918	0.2106	0.7186
C2	0.9327	0.1087	0.7831
C3	0.8517	0.2366	0.7756
C4	0.8287	0.4647	0.7017
C5	0.8888	0.5647	0.6356
C6	0.9701	0.4383	0.6463
C7	0.7473	0.5984	0.6921
C8	0.6761	0.7206	0.6781
C9	0.3056	0.6958	0.8886
C10	0.3090	0.5979	0.7638
C11	0.3562	0.7303	0.6900
C12	0.4013	0.9583	0.7420
C13	0.3981	0.0549	0.8691
C14	0.3492	0.9239	0.9401
C15	0.4515	0.0927	0.6698
C16	0.4972	0.2429	0.6212
H1	0.0548	0.1111	0.7244
H2	0.9518	0.9374	0.8450
H3	0.8062	0.1602	0.8275
H4	0.8689	0.7362	0.5742
H5	0.0168	0.5180	0.5973
H6	0.2696	0.5917	0.9469
H7	0.2716	0.4259	0.7208
H8	0.3571	0.6587	0.5909
H9	0.4370	0.2245	0.9122
H10	0.3458	0.9982	0.0374

Table S4 Optimized cell parameters and atomic coordinates of 3 wt% CNT-P.

Space Group: P1 (C1-1) **a = 12.12 Å α = 84.99°** **b = 19.88 Å β = 89.57°** **c = 8.48 Å γ = 130.68°** **V = 1537.32 Å^3**			
C1	0.8280	0.3911	0.4607
C2	0.5976	0.5193	0.4142
C3	0.3035	0.9344	0.5868
C4	0.8294	0.8200	0.5931
C5	0.7473	0.2406	0.5013
C6	0.7743	0.4910	0.4310
C7	0.0743	0.2458	0.4541
C8	0.9163	0.0829	0.4798
C9	0.0349	0.8191	0.6234
C10	0.5563	0.0774	0.5461
C11	0.3230	0.3930	0.4329
C12	0.8270	0.9300	0.5012
C13	0.7773	0.4916	0.0985
C14	0.8311	0.9303	0.1724
C15	0.3192	0.3941	0.1000
C16	0.8292	0.3911	0.1269
C17	0.0323	0.8146	0.2920
C18	0.0764	0.2462	0.1189
C19	0.3025	0.9349	0.2541
C20	0.5879	0.5016	0.0902
C21	0.5559	0.0770	0.2128
C22	0.9151	0.0827	0.1465
C23	0.7474	0.2402	0.1681
C24	0.1888	0.3272	0.1885
C25	0.8611	0.0027	0.2425
C26	0.1707	0.8737	0.3554
C27	0.4546	0.4538	0.1749
C28	0.8188	0.4497	0.1938
C29	0.4341	0.0026	0.3172
C30	0.8246	0.8611	0.2507
C31	0.9868	0.1634	0.2158
C32	0.6634	0.1581	0.2738
C33	0.7032	0.5141	0.1751
C34	0.9033	0.7688	0.3920
C35	0.8040	0.3200	0.2297
C36	0.8156	0.8603	0.4409
C37	0.7056	0.5159	0.3383

C38	0.8177	0.4489	0.3609
C39	0.4331	0.0019	0.4841
C40	0.8617	0.0040	0.4088
C41	0.9098	0.7931	0.5463
C42	0.4529	0.4504	0.3437
C43	0.6627	0.1576	0.4405
C44	0.9900	0.1651	0.3842
C45	0.1779	0.3358	0.3589
C46	0.1692	0.8720	0.5224
C47	0.8029	0.3193	0.3969
C48	0.4232	0.6317	0.1598
C49	0.3668	0.6472	0.2601
C50	0.3310	0.6861	0.3587
C51	0.1871	0.6378	0.9231
C52	0.1560	0.6752	0.0260
C53	0.2678	0.7602	0.5672
C54	0.4102	0.8100	0.4995
C55	0.4423	0.7736	0.3955
C56	0.8280	0.3911	0.9607
C57	0.5976	0.5193	0.9142
C58	0.3034	0.9344	0.0869
C59	0.8294	0.8200	0.0930
C60	0.7473	0.2406	0.0013
C61	0.7743	0.4910	0.9310
C62	0.0743	0.2458	0.9541
C63	0.9163	0.0829	0.9798
C64	0.0350	0.8191	0.1234
C65	0.5563	0.0774	0.0461
C66	0.3230	0.3930	0.9329
C67	0.8270	0.9300	0.0012
C68	0.7773	0.4916	0.5985
C69	0.8311	0.9303	0.6724
C70	0.3192	0.3941	0.6000
C71	0.8292	0.3911	0.6269
C72	0.0324	0.8146	0.7920
C73	0.0764	0.2462	0.6189
C74	0.3025	0.9349	0.7540
C75	0.5879	0.5016	0.5902
C76	0.5559	0.0770	0.7128
C77	0.9151	0.0827	0.6465
C78	0.7474	0.2402	0.6681
C79	0.1888	0.3272	0.6885
C80	0.8611	0.0027	0.7424
C81	0.1707	0.8737	0.8553

C82	0.4546	0.4538	0.6749
C83	0.8188	0.4497	0.6938
C84	0.4341	0.0026	0.8172
C85	0.8246	0.8611	0.7507
C86	0.9868	0.1634	0.7158
C87	0.6634	0.1581	0.7738
C88	0.7032	0.5141	0.6751
C89	0.9032	0.7687	0.8920
C90	0.8040	0.3200	0.7297
C91	0.8156	0.8603	0.9409
C92	0.7056	0.5159	0.8383
C93	0.8177	0.4489	0.8609
C94	0.4331	0.0019	0.9841
C95	0.8617	0.0041	0.9088
C96	0.9098	0.7931	0.0463
C97	0.4529	0.4504	0.8437
C98	0.6627	0.1576	0.9405
C99	0.9900	0.1651	0.8842
C100	0.1779	0.3358	0.8589
C101	0.1692	0.8720	0.0224
C102	0.8029	0.3193	0.8969
C103	0.4232	0.6317	0.6598
C104	0.3668	0.6472	0.7601
C105	0.3310	0.6861	0.8587
C106	0.1871	0.6378	0.4231
C107	0.1560	0.6751	0.5260
C108	0.2678	0.7603	0.0672
C109	0.4102	0.8101	0.9994
C110	0.4423	0.7736	0.8954
N1	0.1250	0.3890	0.3676
N2	0.6284	0.6069	0.3746
N3	0.1250	0.3890	0.8676
N4	0.6285	0.6069	0.8746
H1	0.1007	0.3859	0.4862
H2	0.0266	0.3545	0.3182
H3	0.7467	0.6712	0.8772
H4	0.6074	0.6107	0.2576
H5	0.1010	0.5708	0.8917
H6	0.0448	0.6374	0.0774
H7	0.4976	0.8768	0.5315
H8	0.1007	0.3859	0.9862
H9	0.0265	0.3545	0.8182
H10	0.7467	0.6712	0.3772
H11	0.6074	0.6108	0.7576

H12	0.1010	0.5708	0.3916
H13	0.0447	0.6374	0.5774
H14	0.4976	0.8768	0.0314
H15	0.2439	0.7862	0.6562
H16	0.5536	0.8109	0.3448
H17	0.2439	0.7863	0.1562
H18	0.5536	0.8109	0.8447
Cu1	0.2672	0.5144	0.2811
Cu2	0.5123	0.6187	0.5063
Cu3	0.2672	0.5144	0.7811
Cu4	0.5123	0.6187	0.0063

Table S5 Control experiment of photocatalytic degradation of naphthalene (10 ppm).

Entry	Cat.	Light	Atmosphere	Scavengers	t[min]	Conv.[%]
1	No	Yes	Air	-	30	5
2	3 wt% CNT-P	No	Air	-	30	7
3	3 wt% CNT-P	Yes	N_2	-	30	6
4[a]	3 wt% CNT-P	Yes	Air	-	30	>99
5[b]	3 wt% CNT-P	Yes	Air	-	30	95
6	3 wt% CNT-P	Yes	O_2	-	10	>99
7[c]	3 wt% CNT-P	Yes	Air	e^-	30	16
8[d]	3 wt% CNT-P	Yes	Air	h^+	30	89
9[e]	3 wt% CNT-P	Yes	Air	$\cdot O_2^-$	30	32
10[f]	3 wt% CNT-P	Yes	Air	$^1O_2$	30	95
11[g]	3 wt% CNT-P	Yes	Air	·OH	30	48

[a]Reaction conditions: substrate (10 ppm), catalyst (10 mg), H_2O (20 mL). [b]Conversion rate after five cycles. [c-g] $Na_2S_2O_8$, CH_3OH, superoxide dismutase (SOD), β-carotene, and isopropanol were added respectively as were used as e^-, h^+, $\cdot O_2^-$, $^1O_2$, and ·OH scavengers.

Table S6 Photocatalytic PHE degradation on reported photocatalyst.

Catalyst	Experimental conditions	PAHs	Removal efficiency (%)	Ref.
A-BC/g-C_3N_4-D	C_{PHE} 1 mg/L, cat. 20 mg, high-pressure sodium lamp (250 W), 320 min	PHE	76.72	[5]
N-doped ZnO-MoS_2	C_{PHE} 25 mg/L, cat. 100 mg, Xe lamp, 120 min	PHE	86.06	[6]
TiO_2/SiO_2-800	C_{PHE} 0.5 mg/L, cat. 20 mg, Xe lamp (450 W), 180 min	PHE	88.00	[7]
CeO_2/FCN	C_{PHE} 5 mg/L, cat. 20 mg, Hg lamp (1000 W), 60 min	PHE	96.60	[8]
Carbon-doped zinc oxide	C_{PHE}=0.2 mg/L, cat. 150 mg, UV lamp (15 W), 60 min	PHE	90.1	[9]
Ag/rGO/BiOBr	C_{PHE}=0.6 mg/L, cat. 100 mg, Xe lamp (500 W), 300 min	PHE	61.6	[10]
P-doped g-C_3N_4/BiOBr	C_{PHE}=1 mg/L, cat. 10 mg, Xe lamp (300 W), 60 min	PHE	99.6	[11]
Mn_3O_4/MnO_2-Ag_3PO_4	C_{PHE}=10 mg/L, Xe lamp, 100 min	PHE	96.2	[12]
TiO_2/titanate nanotube	C_{PHE}=20 mg/L, cat. 20 mg, Xe lamp, 240 min	PHE	95	[13]

3 wt% CNT-P	C_{PHE}=10 mg/L, cat. 10 mg, Xe lamp (300 W), 60 min	PHE	99	**This work**
ZnO/Ag/GO	C_{NAP}=50 mg/L, cat. 250 mg/L, visible light, 50 min	NAP	92	[14]
TiO_2/AC	C_{NAP}=30 mg/L, cat. 400 mg/L, visible light, 120 min	NAP	93.5	[15]
N-TiO_2/ACS-PVP	C_{NAP}=15 mg/L, cat. 100 mg/L, visible light, 100 min	NAP	86	[16]
FeMn/biochar	C_{NAP}=30 mg/L, cat. 1000 mg/L, H_2O_2 (100 mM), visible light, 148 min	NAP	82.2	[17]
Bi_2MoO_6/rGO	C_{NAP}=50 mg/L, cat. 300 mg/L, visible light, 60 min	NAP	95	[18]
Fe_3O_4	C_{NAP}=20 mg/L, cat. 500 mg/L, 480 min	NAP	74.3	[19]
$CeVO_4$	C_{NAP}=30 mg/L, cat. 250 mg/L, visible light, 300 min	NAP	95.1	[20]
3 wt% CNT-P	C_{NAP}=100 mg/L, cat. 10 mg, Xe lamp (300 W), 70 min	NAP	96	**This work**
GO-Fe_3O_4@SiO_2@CdS	C_{PYR}=100 mg/L, cat. 0.1 g/L, 120 min	PYR	93.4	[21]
Ag_3PO_4/MoS_2	C_{PYR}=1100 ug/L, cat. 0.5 g/L, 120 min	PYR	99.4	[22]
3D printed PLA-	C_{PYR}=0.44-3.15 ug/L, UV-	PYR	>94	[23]

TiO_2 composite	light, 24 h			
$Pt/TiO_2/SiO_2$	$C_{PYR}=5\times10^{-8}$ M, UV-light, 10-110 min	PYR	81.4	[24]
TiO_2/quartz fibre filter	C_{PYR}=9.3-196 ng/filter, UV-light, 24 h	PYR	54	[25]
PAM/ZnO PolyHIPE hydrogel composite bead	C_{PYR}=0.17-113.03 ug/L, UV-light, 6 h	PYR	66.74	[26]
3 wt% CNT-P	C_{PYR}=10 mg/L, cat. 10 mg, Xe lamp (300 W), 50 min	PYR	99	**This work**

References

1. F. Kresse, *Phys. Rev. B.*, 1996, **54**, 11169-11186.
2. J. P. Perdew, A. Ruzsinszky, G. I. C. Csonka, O. A. V. Vydrov, G. E. S. Scuseria, L. A. C. Constantin, X. L. Zhou, K. Burke, *Phys. Rev. Lett.*, 2008, **100**, 136406-136409.
3. J. Heyd, G. E. Scuseria, *J. Chem. Phys.*, 2003, **118**, 8207-8215.
4. H. Y. Jiang, P. Zhou, Y. Y. Wang, R. Duan, C. C. Chen, W. J. Song, J. C. Zhao, *Adv. Mater.*, 2016, **28**, 9776-9781.
5. M. Lin, F. Li, W. Cheng, X. Rong, W. Wang, *Chemosphere*, 2022, **288**, 132620-132629.
6. H. A. Chauhan, M. Rafatullah, K. A. Ali, M. F. Umar, M. A. Khan, B. H. Jeon, *J. Water Process. Eng.*, 2022, **47**, 102714-102716.
7. H. Ji, W. Liu, F. Sun, T. Huang, L. Chen, Y. Liu, J. Qi, C. Xie, D. Zhao, *Chem. Eng. J.*, 2021, **419**, 129605-129618.
8. C. J. Feng, J. Rong, Y. Z. Zhang, X. D. Zheng, X. Z. Li, S. Xu, Z. Y. Li, *Appl. Catal. B: Environ.*, 2023, **337**, 123005-123017.
9. Y. Shaban, N. A. Alharbi, Environ. Sci. Pollut. Res., 2022, **29**, 47818-47831.
10. J. Zhao, W. Tian, M. Chu, H. Chen, S. Yang, J. Jiang, *Chemosphere*, 2022, **297**, 134175-134184.
11. Y. Feng, Y. Tao, J. H. Qu, Y. Zhang, *Chem. Eng. J.*, 472 2023, **472**, 145053-145068.
12. H. Y. Cai, L. Sun, Y. M. Wang, T. W. Song, M. T. Bao, L. X. Yang, *Chem. Eng. J.*, 2019, **369**, 1078-1092.
13. X. Zhao, Z. Q. Cai, T. Wang, S. E. O˙Reilly, W. Liu, D. Y. Zhao, *Appl. Catal. B: Environ.*, 2016, **187**, 134-143.
14. N. Mukwevho, R. Gusain, E. Fosso-Kankeu, N. Kumar, F. Waanders, S. S. Ray. *J. Ind. Eng. Chem.*, 2020, **81**, 393-404.
15. D. Liu, Z. Wu, F. Tian, B.C. Ye, Y. Tong. *J. Alloy. Compd.*, 2016, **676**, 489-498.

16. E. H. Doabi, F. Elmi, M. M. Elmi. *J. Photochem. Photobiol. A Chem.*, 2022, **425**, 113677.

17. L. Li, et al. *Water Res*, 2019, **160**, 238-248.

18. F. Li, M. Lin. *Int. J. Environ. Res. Public Health*, 2020, **17**, 2065.

19. J. Zhang, S. Fan, B. Lu, Q. Cai, J. Zhao, S. Zang. *R. Soc. Open Sci.*, 2019, **6**, 181779.

20. G. Lu, B. Song, Z. Li, H. Liang, X. Zou. *Chem. Eng. J.*, 2020, **402**, 125645.

21. T. Li, M. Wang, Y. Hao. *Sci. Total Environ.*, 2023, **857**, 159254.

22. Y. Wang, W. Feng, A. Gong, W. Zhang, L. Qiu, Y. Chen, J. Han. *Catal. Lett.*, 2024, **154**, 3574-3593.

23. A. D. McQueen, M. L. Ballentine, L. R. May, C. H. Laber, A. Das, M. J. Bortner, A. J. Kennedy. *ACS Environ. Sci. Technol. Water*, 2022, **2**, 137-147.

24. Z. H. Luo, C. L. Wei, N. N. He, Z. G. Sun, H. X. Li, D. Chen. *J. Nanomater*, 2015, 284834.

25. K. Sohara, K. Yamauchi, X. Sun, K. Misawa, Y. Sekine. *Catalysts*, 2021, **11**, 1-12.

26. P. Inphak, P. Kaewdee, C. Randorn, C. Thiraphatchotiphum, A. Asanakham, T. Kiatsiriroat, S. Tandorn. *Appl. Catal. B: Environ.*, 2026, **381**, 125825.